# Characterizing the Effects of Land Cover Heterogeneity on Convective Cells and Precipitation in Houston, Texas

**Oluwafemi Omitusa[1,2], David Bodine[1,2]**

[1]*School of Meteorology, University of Oklahoma, Norman, Oklahoma*

[2]*Advanced Radar Research Center, University of Oklahoma, Norman, Oklahoma*

## Introduction

- Urban regions, with their dense infrastructure and activity, exhibit distinct climatic patterns, which can influence atmospheric convection, leading to the formation of convective cells (Han et al., 2014)

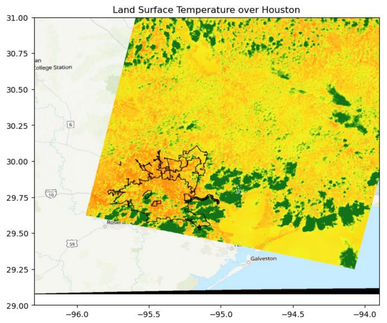


Fig. 1: Average land surface temperature mapping over Houston for summer 2022

- Although the synoptic-scale factors for convection initiation (CI) are well understood (Feng et al., 2022; Torri et al., 2015), our knowledge of the local environmental conditions that influence CI and growth remains limited
- Moreover, despite the progress in understanding the behavior of convective cells in urban regions, there are still limitations in the current knowledge regarding how specific urban features affect convective cell initiation and behavior
- An important research question we seek to answer is: **How do the near-storm characteristics of convective cells vary throughout their lifetime in the urban region compared to the surrounding regions?**

## Methodology

- Convective cells are tracked within the KHGX NEXRAD dataset for the summer months of 2021 and 2022 using PyFLEXTRKR algorithm (Feng et al., 2022)

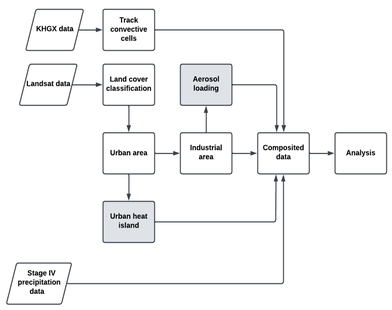


Fig. 2: Flowchart of the methodology

- The cells are identified based on a minimum composite radar reflectivity core of 50 dBZ

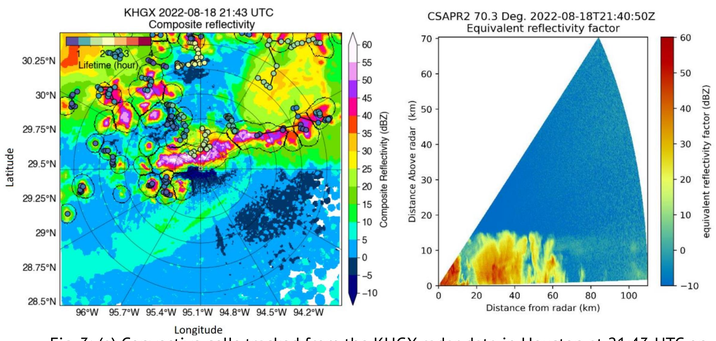


Fig. 3: (a) Convective cells tracked from the KHGX radar data in Houston at 21:43 UTC on August 18, 2022. (b) Cross-section showing the vertical structure from the closest in-time HSRHI scan

- Stage-IV precipitation dataset for the summers of 2021-22 are composited with the tracked convective cells

- Subsequently, the urban area of Houston was extracted and classified using the USFS landscape data
- We define the upwind, urban, and downwind regions of Houston based on Shepherd et al. (2001)'s framework

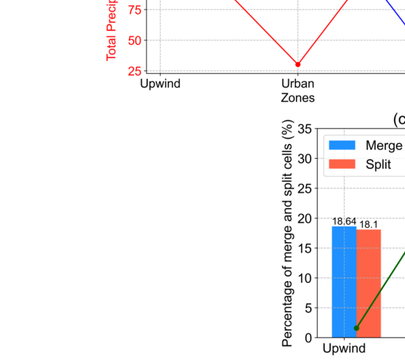


Fig. 5: Coordinate system to define upwind, urban, and downwind regions

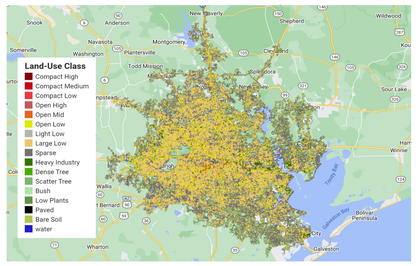


Fig. 4: Local climate zone classification of Houston's urban area

Table 1: Land area of different regions

| Region | Area (km$^2$) |
|---|---|
| Upwind | 17,795 |
| Urban | 8,274 |
| Downwind | 17,840 |
| Left minimal-to-no-impact | 1,649 |
| Right minimal-to-impact | 5,763 |

## Results

### Convective cell characteristics across different regions

- Highest precipitation per cell in the downwind reflects storm intensification away from the coast, potentially influenced by inland dynamics such as urban heat island (UHI) effect and surface roughness

Table 2: Number of convective cells tracked in each region (June-August, 2021-22)

| Cells | All | Upwind | Urban region | Downwind |
|---|---|---|---|---|
| Total | 54,932 | 21,733 | 17,695 | 4,708 |
| Non-merge | 44,961 | 17,642 | 14,247 | 3,858 |
| Merge | 9,971 | 4,091 | 3,448 | 850 |
| Non-split | 45,255 | 17,638 | 14,149 | 3,912 |
| Split | 9,677 | 4,095 | 3,546 | 796 |

- Highest cell density in downwind region suggests possible merging and growth of cells into larger but weak, deep systems
- Cells in the urban region exhibit the greatest intensity, size, and density but are shallower, possibly due to the UHI effect and convergence zones




Fig. 6: Variation of cell characteristics across different regions

### Convective cell characteristics based on development stage

Table 3: Diurnal proportion of cells in different regions at each development stage

| Time of Day | Upwind Region | | | Urban Region | | | Downwind Region | | |
|---|---|---|---|---|---|---|---|---|---|
| | Developing | Dissipating | Mature | Developing | Dissipating | Mature | Developing | Dissipating | Mature |
| Night | 30.7% | 7.2% | 11.9% | 26.8% | **8.6%** | 9.3% | 29% | **13.4%** | **14.3%** |
| Morning | 32.1% | 7.7% | 11.7% | 29.8% | 6.1% | 9.8% | 33.1% | 7.3% | 14.1% |
| Noon | **35.2%** | 7.7% | **12.5%** | 32.2% | 6.7% | **11.3%** | 31.6% | 5.0% | 10.4% |
| Evening | 34.6% | **9.6%** | 11.8% | **34.8%** | **8.6%** | 10.6% | **34.5%** | 7.8% | 10.3% |

All values are statistically significant at the 95% significance level

- Cells in urban and downwind regions typically initiate in the evenings and dissipate during the night

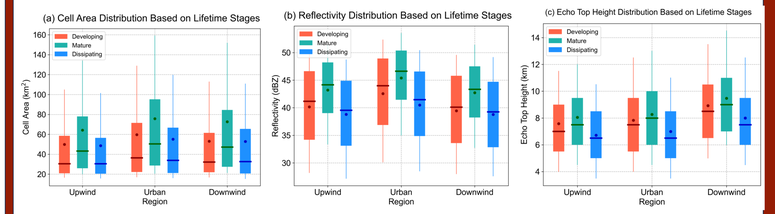


- Throughout their lifetime, urban cells are the most intense and largest while downwind cells achieve the greatest depth
- Around 7 PM, nearly half of all cells are located in the urban region, where they exhibit the most significant weakening
- Cell reflectivity remains relatively constant during morning and afternoon in both upwind and urban regions.
- Cells spend the longest duration in the developing stage and the shortest time in their mature stage

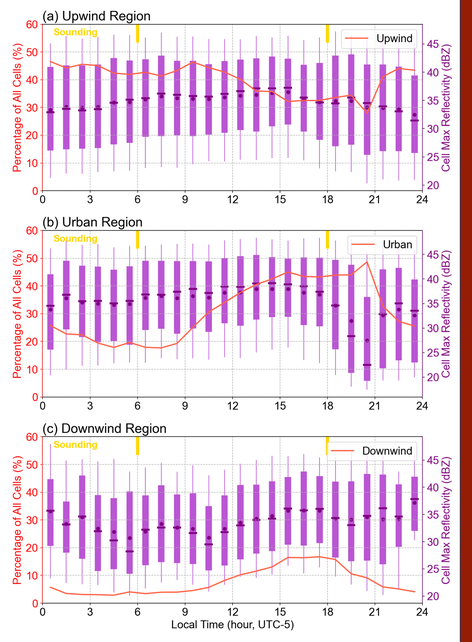


## Conclusions and Future Work

- Overall, urban cells are deeper and larger than those in other regions, indicating the potential impact of urbanization
- Determining whether these observed effects are due to coastal influences or urbanization remains a challenging aspect of the study
- Next steps include analyzing variations in cell characteristics with altitude and conducting a control study for comparative analysis

## References

- Feng, Z., Varble, A., Hardin, J., Marquis, J., Hunzinger, A., Zhang, Z., & Thieman, M. (2022). Deep Convection Initiation, Growth, and Environments in the Complex Terrain of Central Argentina during CACTI. https://doi.org/10.1175/MWR-D-21-0237.1
- Han, J. Y., Baik, J. J., & Lee, H. (2014). Urban impacts on precipitation. Asia-Pacific Journal of Atmospheric Sciences, 50, 17-30
- Shepherd, J. M., Pierce, H., & Negri, A. J. (2002). Rainfall modification by major urban areas: Observations from spaceborne rain radar on the TRMM satellite. Journal of Applied Meteorology and Climatology, 41(7), 689-701
- Torri, G., Kuang, Z., & Tian, Y. (2015). Mechanisms for convection triggering by cold pools. Geophysical Research Letters, 42(6), 1943-1950

## Acknowledgments

The authors thank the US Geological Survey (USGS) for the Landsat datasets, the USDA Forest Service (USFS) Geospatial Technology and Applications Center (GTAC) for the Land cover classification data, and NOAA National Centers for Environmental Information (NCEI) for the radar dataset.

Oluwafemi.Omitusa@ou.edu  oluwafemi-omitusa-606288a